Cerebral Cortex Advance Access published June 7, 2011

Cerebral Cortex
doi:10.1093/cercor/bhr102

Spatiotemporal Effects of Microsaccades on Population Activity in the Visual Cortex of Monkeys during Fixation

Elhanan Meirovithz[1,2], Inbal Ayzenshtat[1,2], Uri Werner-Reiss[1,2], Itay Shamir[1,2] and Hamutal Slovin[1,2]

[1]Gonda Multidisciplinary Brain Research Center and [2]Mina and Everard Goodman Faculty of Life Sciences, Bar-Ilan University, 52900 Ramat Gan, Israel

Address correspondence to Hamutal Slovin. Email: slovinh@mail.biu.ac.il.

During visual fixation, the eyes make fast involuntary miniature movements known as microsaccades (MSs). When MSs are executed they displace the visual image over the retina and can generate neural modulation along the visual pathway. However, the effects of MSs on neural activity have substantial variability and are not fully understood. By utilizing voltage-sensitive dye imaging, we imaged the spatiotemporal patterns induced by MSs in V1 and V2 areas of behaving monkeys while they were fixating and presented with visual stimuli. We then investigated the neuronal modulation dynamics, induced by MSs, under different visual stimulation. MSs induced monophasic or biphasic neural responses depending on stimulus size. These neural responses were accompanied by different spatiotemporal patterns of synchronization. Finally, we show that a local patch of population response evoked by a small stimulus was clearly shifted over the V1 retinotopic map after each MS. Our results demonstrate the lack of visual stability in V1 following MSs and help clarify the substantial variability reported for MSs effects on neuronal responses. The observed neural effects suggest that MSs are associated with a continuum of neuronal responses in V1 area reflecting diverse spatiotemporal dynamics.

Keywords: fixation, nonhuman primate, primary visual cortex, synchronization, voltage-sensitive dye imaging

Introduction

During visual fixation, the eyes continuously and unconsciously make involuntary miniature movements—drifts, tremors, and microsaccades (MSs; Zuber and Stark 1965; Engbert 2006; Collewijn and Kowler 2008; Kagan et al. 2008; Martinez-Conde et al. 2009; Melloni et al. 2009; Rolfs 2009). MSs are the fastest of these eye movements and displace the visual image over the retina. MSs are detected based on their kinematic properties, although the reported values tend to vary across studies (Martinez-Conde et al. 2004, 2009; Engbert 2006; Collewijn and Kowler 2008; Cui et al. 2009; Kliegl et al. 2009). In addition, the rate and pattern of MSs may differ substantially between subjects and are influenced by training history, stimuli, and behavioral tasks (Engbert 2006; Kagan et al. 2008; Otero-Millan et al. 2008; Cui et al. 2009; Martinez-Conde et al. 2009).

The functional role of MSs is still hotly debated (Collewijn and Kowler 2008; Wurtz 2008; Cui et al. 2009; Martinez-Conde et al. 2009; Rolfs 2009). Their importance is unclear, since they rarely appear during natural vision that does not require prolonged fixation (Kowler and Steinman 1979, 1980). One hypothesis is that MSs are involved in controlling eye position during fixation and correct the retinal displacement caused by drifts (Cornsweet 1956; Nachmias 1959; Skavenski et al. 1975; Gur et al. 1997; Engbert and Mergenthaler 2006; Kagan et al. 2008). It has recently been shown that, on a short time scale, MSs increased fixation errors relative to drifts, while, on a long time scale, they reduced fixation errors (Engbert and Kliegl 2004; Rolfs et al. 2004). Others have suggested that MSs play a crucial role in counteracting neural adaptation and visual fading (Riggs et al. 1953; Skavenski et al. 1979; Livingstone et al. 1996; Engbert and Kliegl 2004; Martinez-Conde et al. 2004). This was confirmed in work by Martinez-Conde et al. (2006) who showed that increased MSs production during fixation resulted in enhanced visibility while decreased MSs production led to periods of visual fading. MSs may also help to enhance the discrimination of stimuli with high spatial frequencies (Bridgeman and Palca 1980; Rucci and Desbordes 2003; Rucci et al. 2007) and have been linked to overt and covert attention (Engbert and Kliegl 2003; Rolfs et al. 2004; Engbert 2006; Laubrock et al. 2007; Martinez-Conde et al. 2009; Rolfs 2009). Covert attention biased the directions of MSs toward and/or away from the spatial location suggested by an attentional cue. Importantly, there is accumulating evidence that MSs play a role in the generation of synchronized visual transients that may be significant for visual processing (Martinez-Conde et al. 2000, 2002). Further roles for MSs have been suggested by Martinez-Conde et al. (2004, 2006, 2009), Collewijn and Kowler (2008), and Rolfs (2009).

MSs have been shown to induce neuronal modulation along the visual pathway: in the lateral geniculate nucleus (Martinez-Conde et al. 2002; Reppas et al. 2002), V1 (Gur et al. 1997; Leopold and Logothetis 1998; Martinez-Conde et al. 2000, 2002; Snodderly et al. 2001; Kagan et al. 2008), and extrastriate cortex (Bair and O'Keefe 1998; Leopold and Logothetis 1998). There is a general consensus that the neuronal modulation in V1 is largely due to retinal displacement (Leopold and Logothetis 1998; Bridgeman 1999; Martinez-Conde et al. 2000, 2002; Snodderly et al. 2001; Kagan et al. 2008; Wurtz 2008). However, it is not clear whether the image displacement over the retina caused by an MS generates an equivalent "image displacement" over the retinotopic map in V1.

Indeed, the spatiotemporal activity patterns induced by MSs during stimulated conditions are not well understood. Depending on the characteristics of the visual stimuli and the behavioral task, suppression (Leopold and Logothetis 1998; Bosman et al. 2009; Herrington et al. 2009) or enhancement effects have been reported (Livingstone et al. 1996; Martinez-Conde et al. 2000, 2002; Kagan et al. 2008) or both (Leopold and Logothetis 1998; Snodderly et al. 2001; Kagan et al. 2008; Bosman et al. 2009; Herrington et al. 2009). In all these experiments, the effect of MSs on neural activity was studied during fixation periods while presenting either a small bar with optimal size and orientation for the receptive

field (RF) of the neuron being recorded (Martinez-Conde et al. 2000, 2002; Snodderly et al. 2001; Kagan et al. 2008) or a stimulus much larger than the RF size (Leopold and Logothetis 1998; Bosman et al. 2009). The occurrence of an MS during the presentation of a small bar can cause the neuron's RF to land on the stimulus, to move over it, or to leave it (Martinez-Conde et al. 2000, 2002; Snodderly et al. 2001; Kagan et al. 2008). However, in studies that presented larger stimuli, the RF did not exceed the stimulus boundaries (Leopold and Logothetis 1998; Bosman et al. 2009).

Modulation of activity throughout the visual areas in response to MSs may result from neural synchronization (Leopold and Logothetis 1998; Martinez-Conde et al. 2000). Martinez-Conde et al. (2000, 2002) showed that MSs were better correlated with bursts of spikes than with single spikes, and further suggested that spatiotemporal summation of spikes generated after each MS may indicate synchronization between these neurons. A recent local field potential (LFP) study (Bosman et al. 2009) found that MSs modulate neuronal synchronization in the frequency domain (intertrial coherence) in areas V1 and V4. In both areas, gamma-band synchronization followed MSs with an early decrease and late increase (see also a recent review by Melloni et al. 2009).

Here, we investigated the spatiotemporal patterns of population responses in V1 and V2 induced by MSs while presenting stimuli of different sizes. By varying the stimulus size, we were able to study the dynamic interaction between MSs and the stimulus-evoked neural activity. More specifically, we investigated the MSs effects on a local patch of neuronal activation that was evoked by a small stimulus and the MSs effects on neuronal activation in the entire imaged area that was evoked by a much larger stimulus. We utilized voltage-sensitive dye imaging (VSDI) to record population responses in the visual cortex during fixation periods and stimulus presentation. Using small stimuli, we found that every MS shifted the visual image over the retina, accordingly shifting and updating the neural activation over the retinotopic map of V1 area. MSs executed during presentation of the larger stimulus resulted in an initial decrease followed by an increase in neural activation. Neural modulation was also accompanied by a transient increased neural synchronization immediately after an MS onset. Our findings thus clearly demonstrate a lack of visual stability in V1 following MSs.

Materials and Methods

Behavioral Tasks

Three monkeys (*Macaca fascicularis*, males, 9–12 kg) were trained on 2 different types of behavioral tasks. 1) A fixation task in which the trial started when a small gray fixation point (0.1°) appeared on a gray screen and after a random fixation interval (3000–4000 ms), a local visual stimulus was turned on for a variable duration (Gabor patch or a circled spot parameters specified below). The monkey had to maintain fixation within a small fixation window for an additional interval of 2000 ms and was rewarded only if the trial was successfully completed. The stimulated trials were interleaved with blank trials (blank condition), in which the monkey was fixating but no visual stimulus appeared. 2) A discrimination task in which the monkey was requested to discriminate between 2 types of visual images: contour versus noncontour (contour discrimination task) or colored natural images of a monkey's face versus a scrambled face (face discrimination task). The monkeys were trained to fixate on a small (0.1°) white fixation point displayed against a uniform gray background. After a random fixation interval (3000–4000 ms), a stimulus appeared on the screen for a variable time. The animal maintained fixation until it was given the GO signal (turning off the fixation point and stimulus). The monkeys were requested to indicate the perceived stimulus by performing a saccadic eye movement to the appropriate location (right or left side of the screen) and were rewarded for correct response.

To study the effects of MSs on V1 and V2 neuronal response evoked by the visual stimulus during fixation, we selected MSs that occurred with a latency > 100 ms after stimulus onset and a stimulus duration of at least 200 ms.

Visual Stimuli

Visual stimuli were presented on a 21-inch Mitsubishi monitor at 85 Hz 100 cm from the monkey's eyes. The effects of MSs in stimulated conditions were studied only during the fixation period while the visual stimulus was turned on. We used the following visual stimuli: 1) Small stimuli that evoked local neural activity (Fig. 2, Supplementary Fig. S1): a high contrast Gabor patch (contrast, 100%; orientation (θ), 90°; wavelength (λ), 0.25°; σ, 0.125°) or a yellow dot (0.3°). To verify the results over different retinotopic locations, we varied the eccentricity of the stimuli in different recording sessions: 0.9–2° below the horizontal meridian and 0.5–1° from the vertical meridian. The typical RF size reported for the mean eccentricities (1.6± 0.07°, mean ± standard error of the mean [SEM]) that we used is 0.26° (Dow et al. 1981). Angelucci et al. (2002) reported a summation field of 0.75° for these eccentricities (high contrast stimulus). 2) Larger stimuli that activated the entire imaged area: colored natural images of monkey faces (3.6 × 3.6°) and scrambled versions of these images (Ayzenshtat et al. 2010) or an image of randomly oriented and positioned Gabor matrices (11 × 8°). In a single recording session, we used repetitive presentation of identical stimuli, each trial including a single stimulus presentation. To study the effect of MSs in the absence of a visual stimulus, we analyzed the blank condition in which the animal fixated on a fixation point but no visual stimulus appeared.

Two linked personal computers were used to control and present the visual stimulation, perform data acquisition and control the monkey's behavior. We used a combination of imaging software (Micam Ultima) and the NIMH-CORTEX software package. The system was also equipped with a PCI-DAS 1602/12 card to control the behavioral task and data acquisition. The protocol for data acquisition in VSDI has been described in detail elsewhere (Slovin et al. 2002). To enable analysis of single trials, stimulus presentation and data acquisition were triggered by the animal's heartbeat signal (for the removal of heartbeat signal, see VSDI Basic Analysis below), and each trial was saved in a different file.

Data Analysis

Data analysis was performed over a total of 78 recording sessions in 4 hemispheres of 3 monkeys (Le, Ar, Ch). In each recording session, we analyzed only correct trials that were carefully checked for eye movement and their dynamics. All statistical analyses and calculations were carried out using Matlab software (Ver. 2008b, The MathWorks, Inc.).

Voltage-Sensitive Dye Imaging

All experimental procedures were approved by the Animal Care and Use Guidelines Committee of Bar-Ilan University, supervised by the Israeli authorities for animal experiments and were according to the National Institutes of Health guidelines. The surgical procedure has been reported in detail elsewhere (Grinvald et al. 1999; Shtoyerman et al. 2000; Arieli et al. 2002). Briefly, the monkeys were anesthetized, ventilated, and provided with an intravenous catheter. A head holder and 2 cranial windows (25 mm inner diameter) were bilaterally placed over the primary visual cortices and cemented to the cranium with dental acrylic cement. A craniotomy was performed and the dura mater removed, exposing the visual cortex. A thin and transparent artificial dura made of silicone was implanted over the visual cortex. Appropriate analgesics and antibiotics were given during surgery and postoperatively. The anterior border of the exposed area was 3–6 mm anterior to the lunate sulcus. The center of the imaged area was located 1–4° below the horizontal meridian representation in V1 and 1–2° lateral to the vertical meridian. The size of the exposed imaged area covered ~ 3–4 × 4–5° in the visual field at the reported eccentricities. To stain the cortical surface, we used Oxonol VSD

RH-1691 or RH-1838 (Optical Imaging, Israel). VSDI was carried out using the Micam Ultima system based on a sensitive fast camera providing a resolution of 10^4 pixels and up to a 10 KHz sampling rate. The actual pixel size used varied between 100^2 and 170^2 μm^2 and every pixel summed the neural activity mostly from the upper layers of the cortical tissue, yielding an optical signal representing the population activity of ~320–1000 neurons. The actual temporal sampling rate was 100 Hz (i.e., 10 ms/frame). The exposed cortex was illuminated using an epi-illumination stage with an appropriate excitation filter (peak transmission 630 nm, width at half height 10 nm) and a dichroic mirror (DRLP 650), both from Omega Optical, Brattleboro, VT. To collect the fluorescence and reject stray excitation light, we placed a barrier postfilter above the dichroic mirror (RG 665, Schott, Mainz, Germany).

Detection of MSs

Eye position was monitored using an infrared eye tracker (Dr Bouis Device, Kalsruhe, Germany), sampled at 1 kHz, and recorded at 250 Hz. During the behavioral task, the monkey was requested to maintain fixation on a small fixation point while visual stimuli were presented. Fixation was kept within ±1° throughout stimulus presentation.

It was recently suggested that MSs can be defined as fixational saccades (i.e., any saccade produced while attempting to fixate; Kagan et al. 2008; Otero-Millan et al. 2008; for review, see Martinez-Conde et al. 2009). However, here, we detected MSs during long fixation periods based on their kinematic properties (see Martinez-Conde et al. 2004, 2009). We implemented an algorithm for MSs detection (Engbert and Mergenthaler 2006) on our eye movement measurements. MSs were detected in 2D velocity space using thresholds for peak velocity and a minimum duration. We used relative thresholds computed separately for horizontal and vertical components in units of median-based standard deviations (SDs) (the threshold was set to 6 median-based SDs). This produced an elliptic threshold in 2D velocity space. Additionally, a minimal duration of 3 data samples (or 12 ms) was required; that is, an MS was detected if and only if 3 or more data samples were outside the ellipse defined by the horizontal and vertical threshold. A 50-ms minimal interval between MSs was imposed for defining the subsequent MS.

To avoid contamination from other types of eye movements (e.g., saccades) and to conform to previous studies, we used an upper amplitude limit of 1° and a maximal velocity of 100°/s (see Martinez-Conde et al. 2009). We also set a lower limit for MS amplitude (0.1°) to avoid noise contamination in our eye movement data set. To test the reliability of the algorithm for detection and classification of fast eye movements in our data, we plotted the amplitude and velocity histograms as well as the main sequence (i.e., the relation between peak velocity and amplitude). Figure 1 confirms that most of the detected MSs in our eye movement measurements were positioned along the main sequence. Although it was reassuring to find that the main sequence and MSs parameters fell within previously observed ranges, we could not rule out the possibility that the algorithm either missed MSs, misclassified non-MSs events as MSs, or both. We therefore visualized a large percentage of the MS traces and verified that the detection algorithm did not misclassify. Thus, it is reasonable to assume that only a small percentage of eye movements were misclassified. In addition, Engbert (2006) has specifically discussed the robustness and specificity of the detection algorithm for MSs.

Finally, a recent study investigating the relation between MSs and power enhancement in the gamma-band range in human scalp electroencephalography (EEG) recordings (Yuval-Greenberg et al. 2008) showed that broadband power enhancement is not neuronal in origin. Rather, it is an electrical artifact related to eye movements that produce MSs. These MSs' artifacts are not related to the MSs' effects described here. MSs-related artifacts in the EEG are broadband and simultaneous with the MSs. By contrast, the effects described here were measured using optical imaging based on VSD and preceded or followed the MSs by several tens of milliseconds.

VSDI Basic Analysis

The basic analysis consisted of 3 steps (Shoham et al. 1999; Slovin et al. 2002). 1) First, in order to analyze only brain areas that were well stained and illuminated, we selected pixels which were above 15% of maximal illumination level. 2) To correct for the nonhomogeneous illumination pattern, and because the optical response was proportional to the illumination level, all pixels were normalized to their DC level, which was the average fluorescence level of a given pixel over the first few frames before stimulus onset. 3) Finally, the VSDI data acquisition was triggered on the heartbeat signal of the animal, so that the VSDI signal in the blank condition (stimulus free, fixation only) measured the contribution of the heartbeat pulsation to the VSDI signal (Grinvald et al. 1994; Arieli et al. 1995; Shoham et al. 1999). To remove the heartbeat effect, the average blank condition (i.e., averaging over all blank trials within an imaging session) was subtracted from each stimulus-evoked trial. These procedures eliminated most of the noise due to heartbeat, respiration, and fixation-point effects and allowed calculation of single-condition maps representing the neuronal activation evoked by visual stimuli or MSs.

Retinotopic maps were obtained by presenting high contrast horizontal or vertical white bars (0.5 × 4°) on a black screen at increasing eccentricities while the animal was fixating. Retinotopic locations were verified by presenting small (0.5°) 100% contrast Gabor patches on an isoluminant screen at increasing eccentricities.

Analysis of MS Effects on VSDI Evoked Response in the Stimulated Condition

To study the effect of MSs on a local patch neuronal response in V1, evoked by a small stimulus, we analyzed the VSDI signal starting 100 ms after stimulus onset (This enabled us avoiding the large transient of the evoked response; Fig. 2, Supplementary Fig. S1.). For this analysis, we selected trials according to the following criteria: 1) the VSDI signal showed a clear patch of activation induced by the local stimulus and 2) the MS occurred during stimulus presentation and the kinematic properties of the MS enabled us to visualize the activation displacement within the imaged area (e.g., Fig. 2*A*, Supplementary Fig. S1*A*). Next, in each trial, we fitted 2D Gaussians over the local activation patches: a single 2D Gaussian for each of the pre-MS and post-MS activation patches (e.g., Fig. 2*A*, Supplementary Fig. S1*A*). The 2D Gaussians were manually adjusted for size, orientation, and position. An additional 2D Gaussian was positioned at the intermediate cortical zone between the Gaussians that were fitted to activation patches in the pre- and post-MS displacement, with average parameters of the pre- and post-2D Gaussians (right panel, Fig. 2*C*). To quantify the MS effect on the stimulus-evoked neural activation, 3 VSDI time courses were calculated separately (Fig. 2*C*, red, green, and black curves) by averaging over all pixels within the top 20% of the 3 fitted Gaussians. These time courses were normalized to the averaged pre-MS VSDI signal (activity was averaged between 40 and 10 ms prior MS onset, red trace, Fig. 2*C*).

To evaluate the MS effect on the VSDI response evoked in the entire imaged area by a larger stimulus, we analyzed the VSDI signal starting 100 ms after stimulus onset. This enabled to avoid the large transient of the evoked response (Figs 3–6). To analyze the MS effects, we averaged the VSDI signal over areas V1 and V2 separately and aligned it to the MS onset (e.g., Fig. 3*A*).

Evaluating the MS Shuffled Data for Statistical Significance

To assess the statistical significance of the MS effects on the VSDI response, data were pooled from all trials and compared with the same data when shuffled. We used 2 shuffling techniques. 1) Randomization of MS events over the temporal domain: the timing of MS events was randomized within each trial while preserving the same number of events for each trial (data not shown). 2) We dissociated the MS traces from the VSDI signal traces and then shuffled the MS traces and the VSDI traces. This approach fully preserved the statistical distribution properties of MS timing events (the inter-MS interval distribution was kept identical for the real data and the shuffled data). In both cases, we obtained similar results. We then computed the differential maps by subtracting the shuffled maps from the real data map, after aligning them to MS onset (e.g., Fig. 3*B*).

We used *t*-tests to evaluate the statistical significance of our results as well as the difference between the real and the shuffled data.

Correlation Analysis

To investigate the effect of MSs on synchronization between neural populations during the stimulated condition, we calculated the average

correlation maps (Meirovithz et al. 2010). Briefly, using a sliding window of 80 ms width, Pearson correlation coefficient (CC) was computed between each pixel in V1 and all the other pixels in the imaged area for each trial. The outcome was a correlation matrix for each pixel. Next, we averaged the matrices of all the pixels in V1 across trials to generate an average correlation map, which is the average correlation between pixels in V1 and pixels of the entire imaged area. Large positive, zero, and negative correlation values indicate high synchronization, no synchronization, and desynchronization between V1 pixels and the rest of the imaged area, respectively. The same procedure was repeated with the shuffled data. Differential correlation maps were obtained by subtracting the correlation maps of the shuffled data from the MS average correlation maps (Fig. 7*A*). The temporal effect of the MS on synchronization was examined by computing the mean value of the relevant pixels in the averaged correlation maps, yielding a time course of correlation (Figs 7*B* and 8). Note that the time points of correlation denote the center of the sliding window (e.g., t = 0 ms shows the correlation at time interval ± 40 ms relative to MS onset).

Results

VSDI from V1/V2 areas was obtained from 4 hemispheres of 3 monkeys. Eye movements were measured during the performance of 2 different behavioral tasks involving prolonged fixation and visual stimulation (see Materials and Methods). The present analysis focused on modulation induced by MSs in the population response of the VSDI signal. During the task, the monkeys fixated within a window of ±1° around the fixation point. Fixational eye movements were considered for analysis if they did not exceed the limits imposed by this fixation window. During fixation, the monkeys viewed either a small visual stimulus (e.g., Gabor element, 0.5° size) that induced a local patch of neural activation in the imaged area or a larger stimulus extending over several degrees that evoked neural activation in the entire imaged area (array of Gabor patches or natural images, see Materials and Methods).

MS Characteristics

MSs were detected using an implementation of an algorithm for fast eye movement detection (Engbert and Kliegl 2003; Engbert and Mergenthaler 2006), based on a threshold for peak 2D velocity and a minimum duration (see Materials and Methods). To constrain our analysis to MSs and avoid contamination by larger fast eye movements (i.e., saccades), we set upper limits for the MS amplitude (1°) and the MS velocity (100°/s) (Otero-Millan et al. 2008; Rolfs et al. 2008, for review, see Martinez-Conde et al. 2004, 2009). Most of the eye movements detected in our data fell within these defined constraints (>90% for all monkeys). To confirm the accuracy of the MS detection algorithm, we compared the properties of MSs detected in our experiments with those of earlier studies on MSs in nonhuman primates (Martinez-Conde et al. 2000, 2002; Kagan et al. 2008; Herrington et al. 2009); our results were consistent with the previous results (Fig. 1*A*,*B*). The median amplitudes of MSs detected in the blank condition (fixation, no visual stimulation) in the 3 monkeys were 0.3 ± 0.1, 0.28 ± 0.11, 0.28 ± 0.1° (median ± mad) and their median velocity was 25.4 ± 8.4, 23.3 ± 7.9, 29.0 ± 8.6°/s, respectively (median ± mad).

Previous studies described a linear relationship between saccadic peak velocity and amplitude common to all saccades, including MSs (Zuber and Stark 1965; Bair and O'Keefe 1998; Martinez-Conde et al. 2000, 2002; Engbert and Mergenthaler 2006; Otero-Millan et al. 2008). MSs obeying this relationship

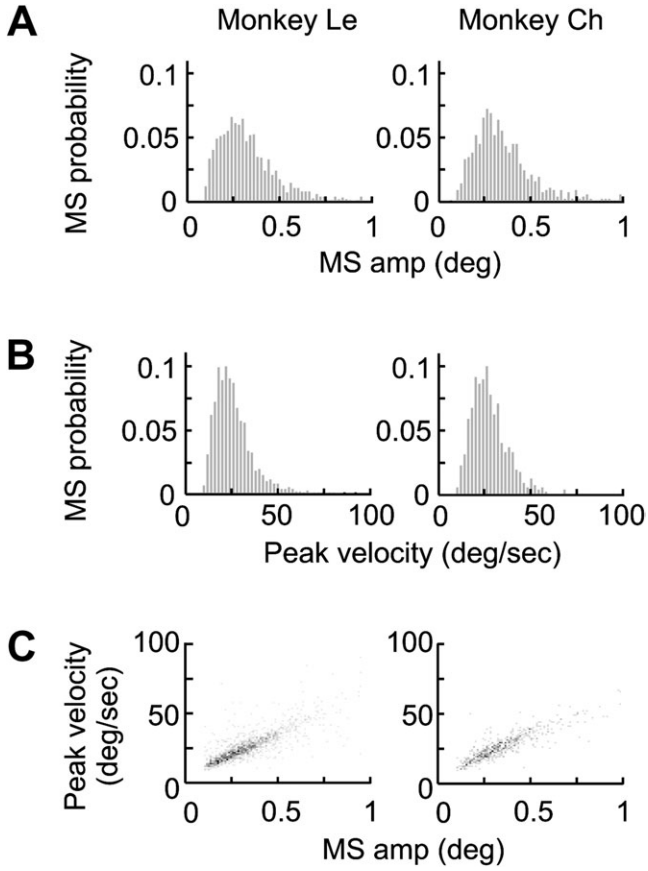

Figure 1. Kinematic properties of MSs. (*A*,*B*) Distribution histograms of MSs amplitude (*A*) and peak velocity (*B*) detected during a prolonged fixation period in the absence of a visual stimulus (blank condition). Lower and upper threshold for amplitude and peak velocity were set to 0.1–1° and 100°/s, respectively. Over 90% of the eye movements of both monkeys were captured within these limits. (*C*) A 2D histogram of MSs amplitude on the *x*-axis and peak velocity on the *y*-axis (i.e., main sequence plot) calculated for the 2 monkeys. Each dot on the graph is in gray scale that codes the normalized frequency of MSs (% MSs). Zero frequency bins are depicted in white and the highest frequency (100%) is depicted in black. Linear regression: monkey Le, $R^2 = 0.64$, $P < 0.001$; monkey CH, $R^2 = 0.7$, $P < 0.001$.

are said to fall along the "main sequence." The MSs detected in our eye movement analysis obeyed this linear relation. Figure 1*C* shows a 2D histogram of the distribution of MS peak velocity and amplitude for all MSs detected during the blank condition. The number of MSs falling in each bin is shown by the gradations of gray; a bin with a frequency of zero is shown white and a bin with the highest frequency is black. The distributions show a strong linear relationship between peak velocity and amplitude [$R^2 = 0.64$, $P < 0.001$ (monkey Le) and $R^2 = 0.7$, $P < 0.001$ (monkey Ch)]. MSs occurred at an average rate of 1.3–1.4 s^{-1} in the blank condition, consistent with previous reports (Bair and O'Keefe 1998; Martinez-Conde et al. 2000, 2002; Engbert and Mergenthaler 2006).

Spatiotemporal Effects of MSs on Local Neural Activation Evoked by a Small stimulus

MSs affect neural activity in early visual areas, and it is generally agreed that this modulation occurs primarily through retinal motion. That is, MSs primarily generate neural responses by displacing the RFs of visual neurons over otherwise stationary stimuli (Livingstone et al. 1996; Martinez-Conde et al. 2000, 2002; Kagan et al. 2008). However, it is not clear whether the

image displacement on the retina caused by an MS generates an equivalent image displacement on the retinotopic map in V1. In particular, the spatiotemporal patterns induced by MSs occurring in stimulated conditions and with small visual stimuli are not fully understood.

To study these questions, our first step was to examine the effects of MSs on the neuronal population response while the monkey was gazing at the fixation point during the presentation of a small Gabor element (0.5°, 100% contrast, see Materials and Methods). We measured the effects of an MS occurring with a minimal delay of 100 ms after stimulus onset to avoid the transient of the evoked VSDI activity. Figure 2*A* shows the spatiotemporal patterns of the VSDI response from a single trial, aligned to a single MS occurring 150 ms after stimulus onset (the MS parameters are shown in Fig. 2*B*). Frames labeled with negative times show the neuronal population response pre-MS onset, whereas frames labeled with positive times show the population response post-MS onset.

Before MS onset, the VSDI response showed a local patch of population activation in V1 evoked by the onset of the small stimulus. After MS onset (t = 0), the patch of neural activity shifted parallel to the vertical meridian toward a more foveal location (more laterally over the cortical surface). This spatial shift of cortical activation corresponded fully to the MS movement properties showing mainly eye position allocation on the vertical axis. The newly generated activation patch appeared at the new cortical position and partially overlapped the previous patch. The post-MS spatiotemporal patterns suggest that the retinal image displacement induced by an MS generated a corresponding displacement of the Gabor representation within the retinotopic map in V1. This result clearly demonstrates the lack of visual stability in area V1, since every MS shifts the visual image over the retina and neuronal

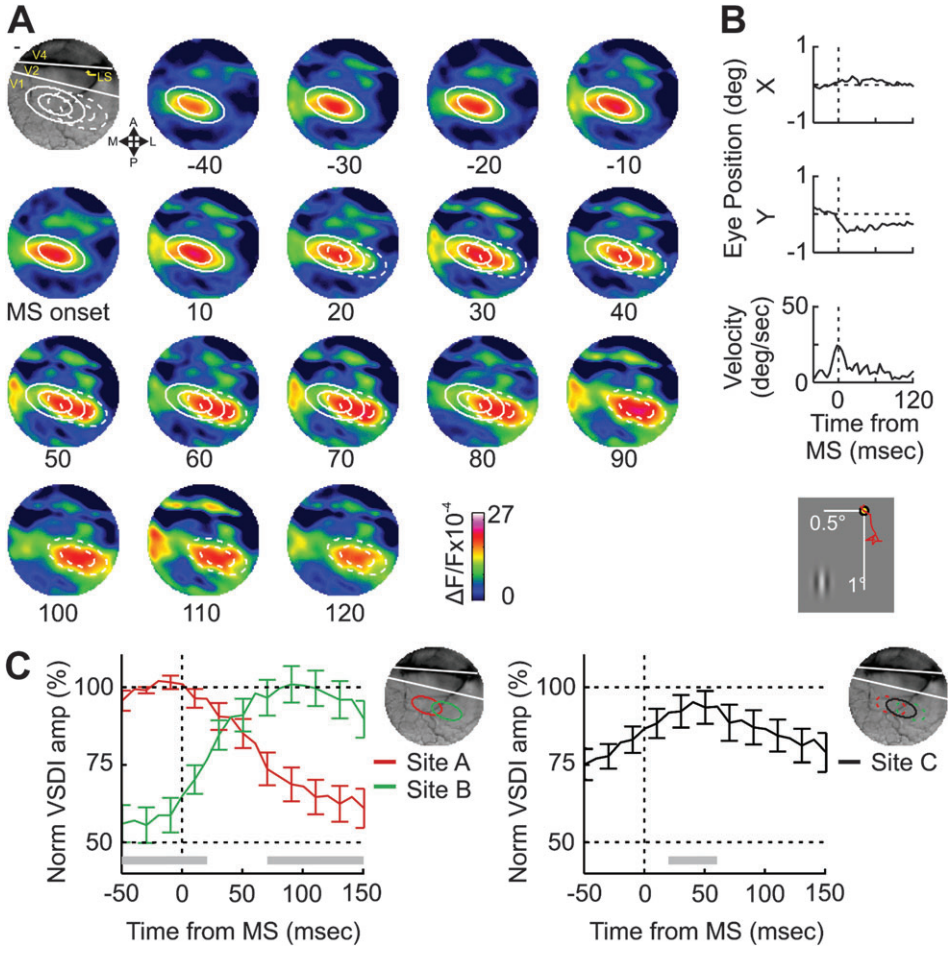

Figure 2. The effect of MSs on neuronal population response in V1 during presentation of a small stimulus. (*A*) A sequence of VSDI activation maps separated by 10 ms from one trial, aligned to the onset of a single MS (t = 0). The MS occurred 150 ms after stimulus onset. Top left panel: blood vessel pattern of the imaged area. The contour lines on the VSDI maps depict the 2D Gaussian fit for the VSDI activation patch: pre-MS activation patch (site *A*) with solid contours and post-MS activation patch (site *B*) with dashed contours. Outer and inner contours depict the top 50% and 20% of VSDI amplitude values. Scale bar, 1 mm. Abbreviations: A: anterior; P: posterior; M: medial; L: lateral. (*B*) Eye position and velocity aligned to the MS during the trial. *X* and *Y* represent horizontal and vertical eye positions, respectively. MS onset is at t = 0. The bottom right panel represents schematic illustration of the visual stimulus (100% contrast; Gabor ($\lambda = 2\sigma = 0.25°$)) and its eccentricity. The yellow dot marks the fixation point and the red trace depicts the eye position during this trial. (*C*) Time course of VSDI signal triggered by MSs and averaged over all trials in 3 retinotopic areas: site A (red curve, left panel), site B (green curve, left panel), and site C show the VSDI response at an intermediate zone located on the MS movement trajectory at the midpoint between site A and site B (black curve, right panel). Time course was calculated for pixels within the Gaussians' top 20% contour and averaged for both monkeys (n = 52; MSs amplitude, 0.43 ± 0.034° [mean ± SEM]; MSs velocity, 37 ± 3.08°/s [mean ± SEM]). Error bars are ±1 SEM. The horizontal gray bars parallel to the abscissa in the left panel denote when the time course at site A was significantly different from that at site B ($P < 0.01$). The horizontal gray bars parallel to the abscissa in the right panel denote when the VSDI time course at site C was significantly different from its baseline (50–10 ms before MS onset activity, $P < 0.05$).

activation is updated accordingly over the retinotopic map in V1 (see also Supplementary Fig. S1).

To quantitatively study, these effects we measured the VSDI responses from multiple trials at 3 cortical sites with fixed coordinates relative to the activation patches (Fig. 2*C*) and then averaged the VSDI responses over trials. Site A shows the VSDI response at the peak of the activation patch occurring pre-MS onset (Fig. 2*C*, left panel, red curve; site A is illustrated schematically by a red ellipse) and site B, the peak of the activation patch occurring post-MS onset (Fig. 2*C*, left panel, green curve; site B is illustrated schematically by a green ellipse). Site C shows the VSDI response at an intermediate zone, located on the MS movement trajectory midway between site A and site B (Fig. 2*C*, right panel, black curve, and ellipse). VSDI response decreased significantly at site A but increased significantly at site B after MS onset ($P < 0.01$, *t*-test). Occurrences of significant differences between sites A and B are marked with a gray bar along the time axis in Figure 2*C*.

Specifically, the VSDI response at site A decreased from 97.5% ± 2.15 (mean ± SEM) at 50–30 ms pre-MS onset to 65.6% ± 5.5 at 100–120 ms post-MS onset ($P < 0.01$, *t*-test). In contrast, the VSDI signal at site B increased significantly from 56.1% ± 5.7 at 50–30 ms pre-MS onset to 98.8% ± 5.6 at 100–120 ms post-MS onset ($P < 0.01$, *t*-test). Figure 2*C* shows that for 20–70 ms post-MS onset, the VSDI responses at sites A and B showed similar amplitudes. The VSDI signal at site C on the MS trajectory showed a much smaller modulation (18%; from 76.3% ± 4.4 at 50–30 ms before MS onset to 94.7% ± 5.4 at $t = 40$ ms after MS onset). The VSDI signal at site A deviated significantly from pre-MS activity at short latency after MS onset, which is earlier than would be expected from the retinal delay, as also found by Kagan et al. (2008). We further address this in the Discussion.

Finally, to give a quantitative estimation about whether the spatial shift along the cortical surface following MS is what one would expect, we performed the following analysis. We computed the expected shift over cortical surface based on the magnification factor as a function of the imaged eccentricities (Tootell et al. 1988; Van Essen et al. 1992; Schira et al. 2007, 2009) and compared it with the actual measured shift over the cortex. We found that the actual shift was similar to the expected (measured shift on the cortex, 4.5 ± 0.33 mm (mean ± SEM); expected shift using the magnification factor, 4.2 ± 0.2 mm; $P = 0.36$, no significant difference; MSs magnitude, 0.51 ± 0.02°; $n = 28$). These results agree with Martinez-Conde (2006) and Kagan et al. (2008) but disagree with Motter and Poggio (1990). We address this further in the Discussion.

Our results help clarify the substantial variability and inconsistent results concerning the effects of MSs on neuronal responses. Because MSs shift the visual image over the retina, they cause dynamic interactions between the visual stimulus and the neuronal activity in the visual cortex. The specifics of this interaction may lead to different activity responses from the recorded neurons (see the VSDI signal in at sites A–C). Previous studies that used local visual stimuli and carefully adjusted the visual stimulus to the RF's size and properties have reported neuronal suppression, neuronal enhancement, or no change of activity in relation to MSs in V1 (Livingstone et al. 1996; Leopold and Logothetis 1998; Martinez-Conde et al. 2000, 2002; Snodderly et al. 2001; Kagan et al. 2008; Bosman et al. 2009; Herrington et al. 2009). Our results indicate that the observed MSs effects depend strongly on the spatial pattern of the stimulus-evoked activity in V1.

Spatiotemporal Effects of MSs on Neural Activation Evoked over the Entire Imaged Area by a Large Stimulus

We next studied the effects of MSs on the neuronal population when the monkeys were gazing at the fixation point and a larger stimulus was presented, activating the entire imaged area (see Materials and Methods). We measured the effects of MSs occurring with a minimal delay of 100 ms after the stimulus onset to avoid the transient of the evoked VSDI response.

The effect of MSs during the presentation of a large stimulus on the VSDI signal from V1/V2 differed substantially from the response to the small local stimulus (Figs 3 and 4, a single recording session and the VSDI signal averaged across all recording sessions, respectively). Now MSs showed a biphasic effect on neural activity in V1 (averaged across all pixels in V1)—an initial decrease followed by an enhancement of neural

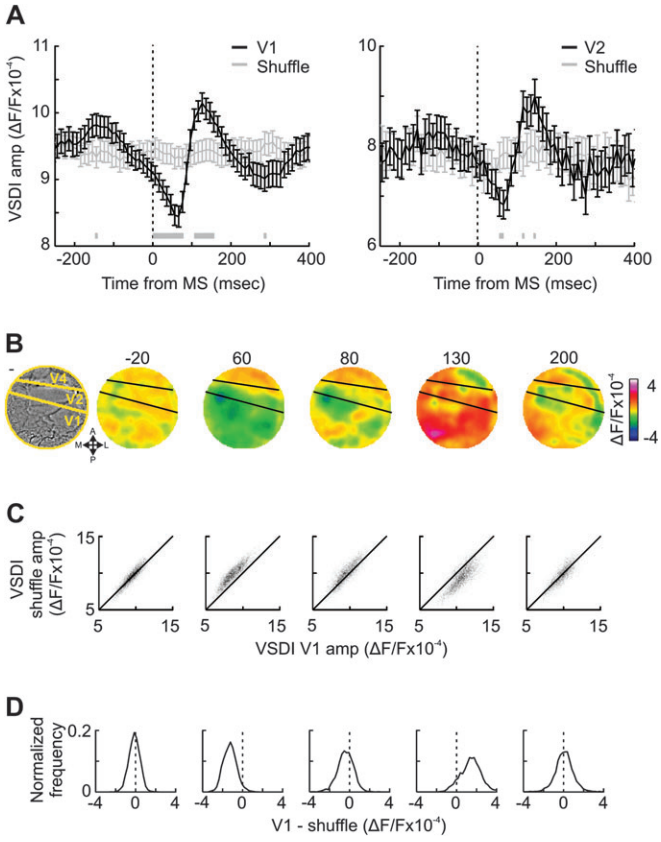

Figure 3. Spatiotemporal patterns of VSDI response induced by MSs in V1 and V2 in the presence of a large stimulus. Data from a single recording day in one monkey ($n = 108$ MSs). The population response over the entire imaged area was evoked by a large visual stimulus (a randomly oriented and positioned Gabor matrix). (*A*) Time course of activation in V1 and V2 areas. The response in both areas is biphasic, first decreasing, and then transiently increasing. Black trace denotes real data, gray trace the shuffled data, error bars are ±1 SEM. Horizontal gray bars parallel to the abscissa denote when the real data and the shuffled data were significantly different ($P < 0.01$). (*B*) Spatiotemporal patterns induced by MSs. Maps were calculated by subtracting the shuffled data maps from the real data maps and the difference averaged over 3 successive frames (i.e., over 30 ms). The time shown above the map depicts the time of the mid-frame. Scale bar, 1 mm. (*C*) Comparing real and shuffled data from V1 pixels ($n = 3364$) in a 2D histogram with real V1 amplitude on the *x*-axis and shuffled amplitude on the *y*-axis. Each dot in the graph is in a gray scale coding the normalized amplitude frequency of the pixels. Zero frequency bins are shown in white and the highest frequency (normalized to 100%) in black. (*D*) Histogram distribution of the difference values between VSDI amplitude in V1 (i.e., real data) and shuffled data in *C*.

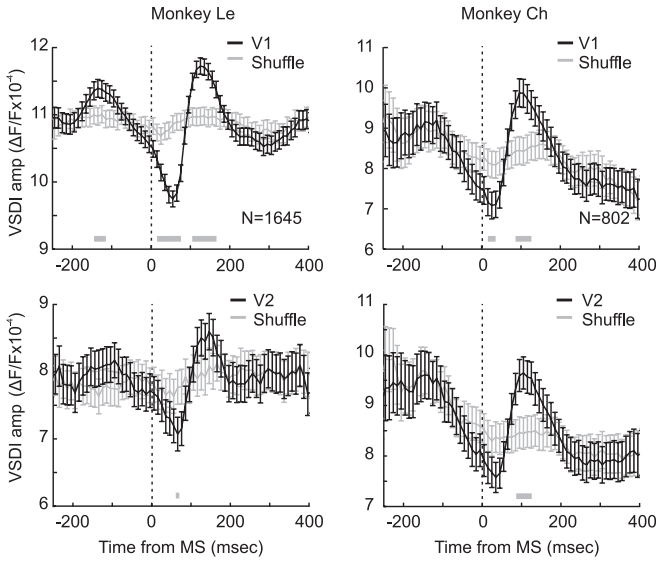

Figure 4. MS effect on VSDI response in the presence of a large stimulus, averaged over all recording sessions. The time course of the VSDI signal aligned to MS onset, averaged across multiple imaging sessions for monkey Le (n = 29 sessions, left panels) and monkey Ch (n = 13 sessions, right panels). As in Figure 3, a large stimulus activated the entire imaged area (left panels, a randomly oriented and positioned Gabor matrix; right panels, natural images of monkey faces). Time course was computed by averaging over pixels in V1 (upper panels) and pixels in V2 (lower panels) for monkeys Le and Ch, respectively. Total number of MSs is n = 1645 (monkey Le) and n = 802 (monkey Ch). The temporal pattern mainly shows a transient decrease of neural activity after MS onset, followed by a transient increase. Real data in black curve and shuffled data in gray curve. Error bars, ±1 SEM. Horizontal gray bars parallel to the abscissa denote a statistically significant difference between the real data and the shuffled data ($P < 0.01$).

population activity (Fig. 3*A*, left panel; Fig. 4, top panels). A similar biphasic VSDI response to MSs was generated in the presence of either large stimulus: Gabor matrices (Fig. 4, left panels) or natural faces (Fig. 4, right panels). To estimate the significance level of the MS effect on the VSDI signal, we computed the shuffled data by shuffling MS traces and traces of the VSDI signal (see also Materials and Methods). Using this method, the inter-MS interval distribution was kept identical for the real data and the shuffled data. Figure 3*A* shows the VSDI signal aligned to MS onset during presentation of the large stimulus (black curve) and the shuffled data (gray curve). This analysis shows that the VSDI signal decreased significantly ($P <$ 0.01) by 11% at t = 60 ms after MS onset and increased significantly by 9% at t = 120 ms after stimulus onset ($P < 0.01$). The same results were obtained by averaging across all recording sessions (Fig. 4). The VSDI signal aligned to MS decreased significantly ($P < 0.01$) by 9% and 12% at t = 50 and 20 ms post-MS onset for monkey Le and Ch, respectively. This was followed by a significant increase ($P < 0.01$) of 7% and 16% at t = 120 and 90 ms post-MS onset for monkey Le and Ch, respectively. Similar results were obtained when we compared the VSDI signal aligned on the MSs, with the VSDI signal without any MSs as a control (Supplementary Fig. S5).

Although the averaged response over all the pixels in V1 shows a biphasic response, it is possible that individual sites in V1 show other responses that merge into a biphasic time course of response after spatial averaging (over all sites in V1). To test this we analyzed MSs in single trials, during the presentation of a Gabor matrix (Supplementary Fig. S2). The VSDI signal before the MS shows clear patches of activation corresponding to the Gabor elements. Following an MS, the Gabor activation pattern was shifted over the cortical surface. We inspected the VSDI response time course at different sites on the cortical surface and found different types of VSDI responses. Thus, the biphasic VSDI response to our large stimuli reflects spatial averaging of local VSDI responses with different dynamics. We further refer to this in the Discussion.

The VSDI response in V2 showed very similar dynamics to those in V1 (Fig. 3*A*, right panel; Fig. 4, bottom panels) but was statistically less significant. Leopold and Logothetis (1998) similarly showed that neuronal activity in V2 increased after MS onset. Averaging the data from all recording sessions shows that the VSDI response in V2 lagged behind V1 by 4–10 ms (Supplementary Fig. S3), further indicating that a significant part of the MS effect results from retinal motion.

The VSDI signal started to decrease before the onset of an MS, despite the continuous presentation of the visual stimulus (the shuffled data showed that part of the segments of this decrease were not statistically significant; Figs 3 and 4). These results fit previous reports of pre-MS modulation of neuronal activity in visual areas (Leopold and Logothetis 1998; Martinez-Conde et al. 2002; Bosman et al. 2009; for saccades: Purpura et al. 2003; Rajkai et al. 2008). There are few suggestions for explaining pre-MS modulation: rhythmic behavior of MSs, extrastriate modulation, neural adaptation, or visual fading. Bosman et al. (2009) have shown in a careful analysis that rhythmic behavior (3–4 Hz) of MSs can induce pre-MS modulation in neuronal activity. To test whether MSs in our data showed rhythmic behavior, we computed the intersaccadic-interval distribution. This was found to be nonhomogenous, with a mean value around 220 to 230-ms interval (Supplementary Fig. S4). We then divided the MS data set into MSs separated by shorter or longer time intervals. The pre-MS modulation was strongly dependent on the interval between successive MSs (e.g., the VSDI signal for longer intervals not showing the decrease just before MS onset.)

Figure 3*B* shows maps of spatiotemporal patterns induced by MSs over the entire imaged area. The suppressed VSDI signal measured at 60 ms after stimulus onset (green pixels) appeared over most parts of V1 and V2 areas. The enhanced VSDI signal measured at 130 ms after MS onset (red-pink pixels) also appeared in most of the V1 and V2 areas. Figure 3*C* shows a sequence of 2D histograms: the VSDI amplitude of each pixel in V1 for the real data versus the amplitude of the shuffled data at the time frames shown in Figure 3*B*. The diagonal represents equal amplitude values in the real data and the shuffled data for every pixel in V1. Figure 3*C* shows that the pixels in V1 covaried in their amplitude when compared with the shuffled data (see also Fig. 3*D*). This result may be simply explained by our use of a large stimulus that activated all the neurons in the imaged area before and after the onset of an MS.

We next studied the relation between MS amplitude and the MS-induced VSDI modulation (Fig. 5). To quantify this relation, we defined a modulation index as the difference between the minimal and maximal amplitude of the VSDI signal after MS onset (Fig. 5*A*; there was no significant difference between the MS amplitude traces before MS onset). We found a linear relation between the modulation index and the MS size; that is, larger MSs induced a larger modulation depth in the VSDI signal (Fig. 5*B*; monkey Le, $R^2 = 0.85$, $P < 0.001$; monkey Ch, $R^2 = 0.73$, $P < 0.003$). Similar results were obtained with the derivative of

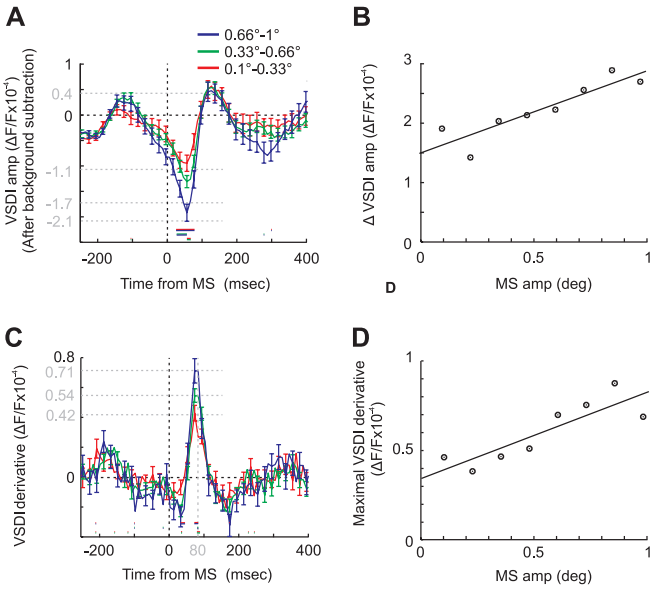

Figure 5. The relation between MS amplitude and VSDI modulation. (*A*) VSDI signal triggered by MS onset ($t = 0$) and sorted by MS size. VSDI background amplitude (i.e., the mean VSDI signal before MS onset: −200 to −100 ms) was subtracted from the VSDI response. Error bars are ±1 SEM. (*B*) The relation between VSDI modulation and MS size. VSDI modulation was computed as the difference between the minimal and maximal VSDI response amplitude after MS onset. The neuronal modulation increased linearly with the MS size, $R^2 = 0.85$, $P < 0.001$; MS size was binned to 0.125°, except for the first bin that was 0.1°. Visual stimulation as in Figure 3. (*C*) The derivative of the VSDI signal aligned on MSs onset ($t = 0$) and sorted by MSs size. Error bars are ±1 SEM. (*D*) The relation between VSDI derivatives and MS size. The maximal VSDI derivatives increased linearly with the MS size, $R^2 = 0.83$, $P < 0.001$; MS size was binned to 0.125°, except for the first bin that was 0.1°. Visual stimulation as in Figure 3. Data from monkey Le. Horizontal bars parallel to the abscissa denote time of significant difference between any pair of the different curves ($P < 0.01$), color coded by the curves' color.

the VSDI signal, aligned on MS onset (Fig. 5*C*,*D*; monkey Le, $R^2 = 0.83$, $P < 0.001$; monkey Ch, $R^2 = 0.79$, $P < 0.02$). This result agrees with previous studies (Armington and Bloom 1974; Dimigen et al. 2009; Tse et al. 2010) and may be due to larger MSs causing the image to shift faster over the retina, making the visual stimulus less effective in driving V1 neurons. That is, the VSDI signal would decrease as a function of MS amplitude; when the eye becomes stationary the signal would increase back to its previous level as stimulus information again streams into the visual cortex.

Finally, we compared the stimulus-evoked VSDI response with the MS effect (Fig. 6). The time of maximal evoked response and the time of maximal enhancement are similar (~120 ms after visual stimulus or MS onset). The MS amplitude modulation is 22% relative to the evoked response. Similar results were obtained when comparing the VSDI signal at baseline before an MS (i.e., the stimulus-evoked VSDI signal) with the MS amplitude modulation (amplitude modulation is 20–30% relative to VSDI baseline activity at 250–200 before MS onset, Figs 3 and 4).

MSs Induce Patterns of Synchronization within the Neuronal Population

The data presented in Figures 3 and 4 suggest that MSs induce covariation in the activity of a large neuronal population in V1 and V2. To investigate this effect, we calculated the Pearson CC between each of V1 pixels and all the pixels in the imaged area (see Materials and Methods) for trials with the large stimulus

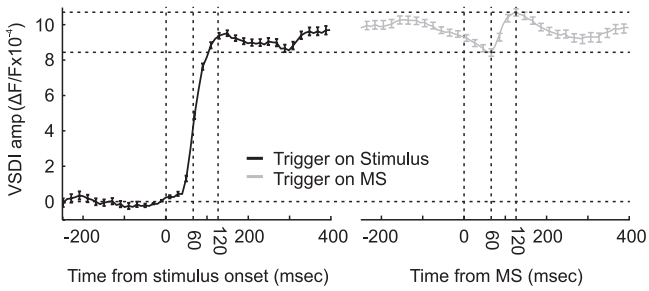

Figure 6. The stimulus-evoked VSDI response and the MS effect. The stimulus-evoked VSDI signal and the MS effect on the VSDI signal. The black trace denotes the VSDI signal aligned on stimulus onset ($t = 0$). The gray trace denotes the VSDI signal aligned on the MS ($t = 0$). Error bars are ±1 SEM. Data are shown for a single recording day in one monkey (150 trials, 108 MSs; data from Fig. 3, large stimulus presentation).

presentation. This was calculated for each trial and then averaged across trials to create an averaged spatial correlation map of the VSDI response triggered by an MS. The same procedure was repeated with the shuffled data. Differential correlation maps were obtained by subtracting the correlation maps of the shuffled data from the real data. The differential correlation maps in Figure 7*A* represent the average CC values between V1 pixels and the pixels in the entire imaged area at specific times in relation to MS onset in a single recording session. It is clear that the MS induced an increased correlation over large parts of the V1- and V2-imaged areas (red/pink pixels), indicating synchronization over a large neural population. In addition, at times before and after this transient increased synchronization there was a slight decrease in neural synchronization relative to the shuffle data (green pixels).

Next, we calculated the time course of correlations averaged over pixels in V1 area (Fig. 7*B*) for the recording session in Figure 7*A*. Figure 7*B* shows a significant transient increase in correlation of 75% (relative to the shuffle data) shortly after MS onset (t = 100 ms after MS) that lasted 50 ms. Averaging over multiple recording sessions using 2 different visual stimuli gave the same result (Fig. 8*A*). There was a significant transient increase in correlation shortly after MS onset (t = 90 and t = 60 ms after MS onset, 64% and 77% from the shuffled value for monkey Le and Ch, respectively) that lasted for 50–70 ms. Similar results were obtained when we used the VSDI signal without MSs as a control (Supplementary Fig. S5). The increased correlation after MS onset is consistent with recent studies showing that MSs induce a burst of spikes in V1 neurons (Martinez-Conde et al. 2000, 2002). As the maximal correlation values in Figures 7 and 8 are rather small, we tested whether this result was due to endogenous fluctuations in the cortex or a simple signal-to-noise limitation. To do this, we spatially smoothed the functional images and then spatially resampled them, so that the correlation was computed between pixels with higher signal-to-noise activity (Supplementary Fig. S6). This increased the absolute value of correlation for the real data, shuffled data, and their difference at the time of correlation peak (the difference in correlation was doubled). This analysis suggests that the correlation values we measured are limited also by signal-to-noise ratio.

Before and after the increased synchronization there was a slight decrease in neuronal synchronization compared with the shuffled data (Fig. 7*B*). Similar results were obtained when averaging over multiple recording sessions (Fig. 8*A*).

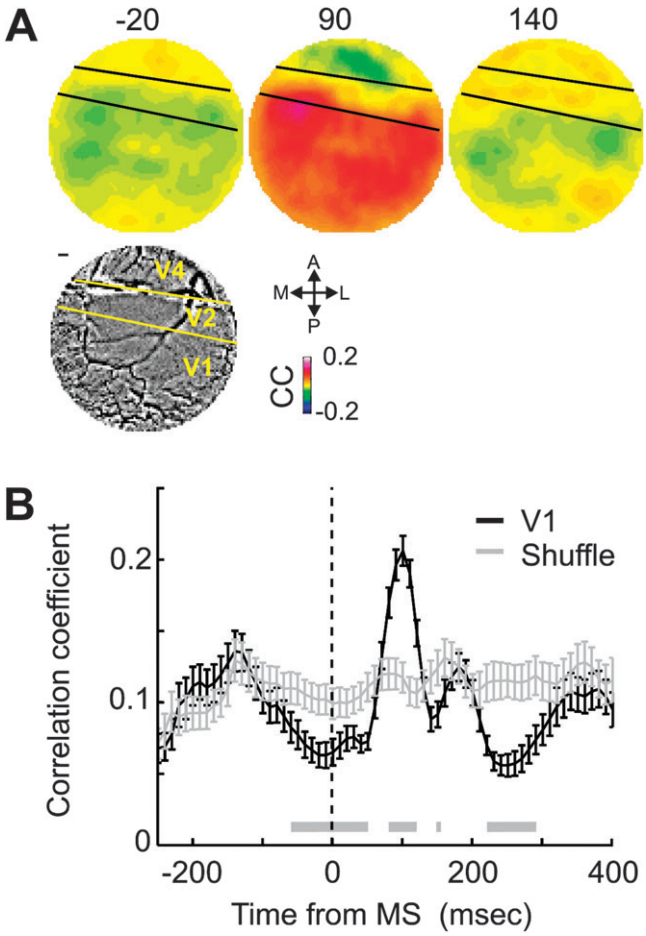

Figure 7. The effect of MSs on population synchronization in the presence of a large stimulus. (*A*) Mean differential spatial correlation maps of all pixels in V1 (correlation map of the shuffled data was subtracted from the real data; for details, see Materials and Methods). The maps show the correlation values for V1 and V2 calculated using an 80 ms sliding window. The maps are depicted for time points: −20, 90, and 140 ms relative to MS onset ($t = 0$). Each map was averaged over 3 sequential time windows. Scale bar, 1 mm. (*B*) The correlation time course in V1 pixels was calculated by averaging the CC over V1 pixels. Note that the time points denote the center of the sliding window (e.g., $t = 0$ ms shows the correlation at time interval ± 40 ms relative to MS onset). Black trace shows real data; gray trace shows shuffled data. Error bars, ±1 SEM. Horizontal gray bars parallel to the abscissa denote when there was a statistically significant difference between the real and the shuffled data ($P < 0.01$). Visual stimulation as in Figure 3.

Finally, we computed the time course of correlations of the VSDI response triggered by MSs during presentation of the small visual stimulus (Fig. 8*B*) at sites A (pre-MS activation patch) and B (post-MS activation patch). There was an early increase in synchronization at the pre-MS activation patch (site A, an increase of 66%, t = 10 after MS onset) followed by an increased synchronization at the post-MS activation patch (site B, an increase of 45%, t = 50 after MS onset). Increased synchronization in the VSDI signal reflects increased common dynamic changes between neuronal populations (i.e., pixels; see Discussion). The early increase in synchronization was related to the decreased response in the pre-MS activation patch (Fig. 2*C*, red curve) and the later increase in synchronization was related to the increased VSDI signal in the post-MS activation patch (Fig. 2*C*, green curve). These results demonstrate distinct spatiotemporal synchronization patterns that are dependent on the stimulus-evoked neuronal response and the MS.

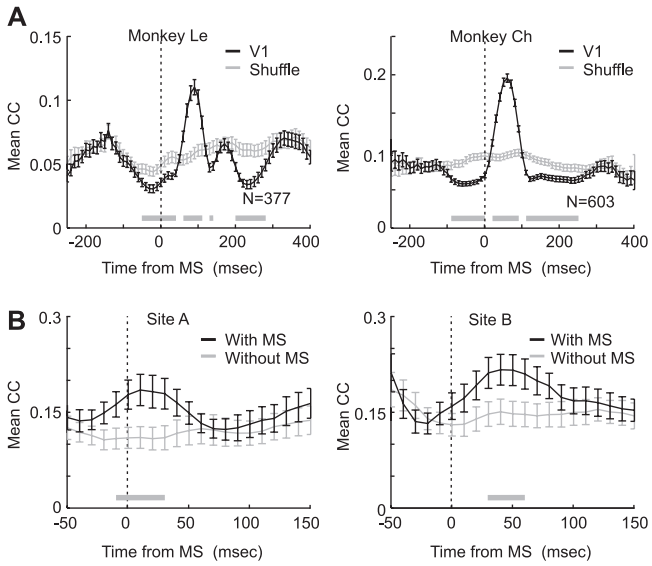

Figure 8. MS effect on population synchronization averaged over all recording sessions. (*A*) Average correlation over all trials (large stimulus) calculated for 2 monkeys (monkey Le, $n = 377$, MSs; monkey Ch, $n = 603$, MSs). Black curve shows real data, gray curve, the shuffled data. Horizontal gray bars parallel to the abscissa denote when there was a statistically significant difference between the real and the shuffled data ($P < 0.01$). We used a large visual stimulus that activated the entire imaged area (left panels: a randomly oriented and positioned Gabor matrix; right panels: natural images of monkey faces). (*B*) Time course of average correlation for trials with local stimulus presentation. The time course was averaged over all trials at sites A and B (as in Fig. 2) corresponding to the center of the activation patch before and after MS onset. Black trace shows real data (VSDI triggered by MSs) and gray trace shows VSDI data without MSs. The CC was averaged from 2 monkeys ($n = 52$, MSs). Horizontal gray bars parallel to the abscissa denote when there was a statistically significant difference between real data and the VSDI data without MSs ($P < 0.01$). Error bars, ±1 SEM in all panels.

Discussion

VSDI was used to measure neuronal population responses from V1 and V2 in monkeys during fixation and visual stimulation. The kinematic properties of the detected MSs fell well within the previously reported range (Engbert 2006; Collewijn and Kowler 2008; Otero-Millan et al. 2008; Martinez-Conde et al. 2009; Rolfs 2009). We investigated the dynamics of the neuronal modulation of visual responses induced by these MSs.

MSs induced monophasic or biphasic modulation in the population activity (averaged over V1 pixels) depending on stimulus size. This modulation was accompanied by different spatiotemporal patterns of synchronization. In addition, we showed that a local patch of population response evoked by a small stimulus was clearly shifted over the retinotopic map of V1 after each MS. Our results clearly demonstrate the lack of visual stability during different visual stimulation.

MS Effects on Local Neuronal Activity Evoked by a Small Visual Stimulus

Previous studies in V1 have suggested that the main effects of MSs arise from the image shifting over the retina (Livingstone et al. 1996; Martinez-Conde et al. 2000, 2002; Snodderly et al. 2001; Kagan et al. 2008). However, the reported neural responses vary considerably across different studies, making it difficult to generalize.

Snodderly et al. (2001) and Kagan et al. (2008) categorized the neurons in V1 into 3 classes according to whether MSs

shifted the RF onto the stimulus, off the stimulus, or across the stimulus. According to their findings, 1) Position (drift) cells were activated when their RF shifted onto the stimulus and remained activated during the intersaccadic periods as long as the neuron's RF was on the stimulus. Alternatively, if the MS shifted the RF off the stimulus, neural activity was suppressed to baseline. Shifting the RF across the stimulus resulted in no significant activity. They categorized 39% of the modulated neurons as position cells. 2) Saccadic cells that were transiently activated at all 3 RF displacement alternatives (~25% of the modulated neurons). 3) Mixed cells that responded at all displacement alternatives as well as showing sustained activation during intersaccadic periods while the neuron's RF was on the stimulus (~36% of the modulated neurons).

Our results are basically consistent with these observations and further suggest that MSs are associated with a continuum of neuronal responses in V1 area reflecting diverse spatiotemporal dynamics (Fig. 2). By utilizing VSDI, we directly imaged the spatiotemporal patterns induced by MSs when a local stimulus was presented and our VSDI responses largely overlap with the specific neuronal categories suggested by Kagan and Snodderly. We showed that MSs generated a delayed sustained decrease at the pre-MS activation patch or a sustained delayed increase of VSDI response at sites A (pre- at the post-MS activation patch) and B (post-MS activation patch), respectively (Fig. 2), which is in accordance with the reported responses of position cells. As one would expect, moving the position cells' RF off the stimulus or onto the stimulus resulted in delayed decreased or increased activity. The VSDI response to MSs that we observed at site C (the intermediate zone) may reflect the responses of the mixed cells or a combination of the saccadic cells with the position cells. The response at the intermediate zone peaked earlier than that at pre- and post-MS zones, reminiscent of the difference in delay between position and saccadic/mixed cells of Kagan and Snodderly. We did not observe a clear transient VSDI response that could link it directly with saccadic cells, possibly due to the VSDI averaging over multiple neuronal responses, whereas Snodderly and Kagan recorded single and multiunits. In addition, only 25% of the modulated cells were saccadic cells, thus having relatively small contribution to the population response.

The shift of neuronal activity over the cortical surface due to an MS was similar and not significantly different from that expected from the magnification factor. This result differs from that of Motter and Poggio (1990) who measured the positions of RF borders in V1 of awake monkeys during attentive fixation. The RF border position, marked by the onset of activity evoked by a moving stimulus, showed less variability than expected from previous measurements of eye position variability during fixation. The discrepancy may be due to our studying the VSDI response to real MSs, whereas Motter and Poggio used a moving bar that crossed the RF of V1 neurons during attentive fixation. The perceptual outcomes of stimulus movement due to MSs or due to a bar moving over the screen are quite different. Whereas the visual image is stabilized despite its displacement by an MS, the motion of a bar moving over the screen is well perceived. The movement of the bar could also have generated motion signals or top-down influences reducing the expected variability.

The VSDI signal at site A, deviated significantly from pre-MS activity at very short latency after MS onset, which is earlier than would be expected from the retinal delay, as also found by Kagan et al. (2008, their Fig. 3). A possible explanation for this can be extraretinal influences (Kagan et al. 2008) that were reported to precede the MS onset. Another possible explanation is related to lateral spread (Slovin et al. 2002) of the VSDI signal (evoked by the previous onset of the local stimulus) to nearby sites (i.e., site B in Fig. 2). This spatial spread is mediated by horizontal connections at relatively slow propagation velocity. In addition, the VSDI signal emphasizes subthreshold population activity and is highly sensitive to the horizontal spread, whereas most previous MS studies have been using spiking activity that is much less sensitive to these aspects of neural activity.

Our results indicate that in the first 100 ms after MS onset there are salient neuronal response changes in V1 which are not perceived. In fact, the first 100 ms after MS onset is a period of perceptual ambiguity (e.g., the simultaneous increase and decrease of the VSDI signal at sites A and B, Fig. 2). This further suggests that V1 cannot be used to directly update visual perception during these brief time periods, and that a spatiotopic map in another area may be more useful to fill-in the gap (Wurtz 2008). Finally, we note that although we focused on the dynamical effects of MSs on neural population in the presence of visual stimulation others have reported extraretinal influences in relation to MS (Snodderly et al. 2001; Kagan et al. 2008) although these effects were variable over different animals.

MS Effects on Neural Activity When RF Is Shifted within the Boundaries of a Large Stimulus

In contrast to MSs occurring during presentations of a small stimulus, where the recorded RF can land on stimulus, move over it or leave it (Martinez-Conde et al. 2000, 2002; Snodderly et al. 2001; Kagan et al. 2008), for larger visual stimuli, MSs shift the RFs within the stimulus boundaries (Leopold and Logothetis 1998; Bosman et al. 2009). We showed that MSs during the presentation of a large visual stimulus induced a biphasic response (when averaged over V1 pixels), suppression followed by enhancement, consistent with results from other studies using stimuli larger than the recorded RF (Leopold and Logothetis 1998; Bosman et al. 2009). MacEvoy et al. (2008) showed that large images induce common lateral suppression. Surprisingly, less suppression (~100 ms after saccade onset) was observed for stimuli entering RFs with saccades compared with flashed stimuli. These results may point to a facilitation starting ~100 ms after an MS. The decrease in VSDI signal within the first 100 ms after MS onset may reflect the displacement of the stimulus over the retina but may also be related to suppressed perception, that is, MSs suppression (Ditchburn 1955; Beeler 1967; Herrington et al. 2009; Martinez-Conde et al. 2009). The transient response increase, about 100 ms post-MS, may reflect a phase of reprocessing and enhanced perception.

Although the VSDI response to small and large stimuli (for the large stimulus, the VSDI response is averaged over all V1 pixels) is different, we cannot exclude the possibility that this effect may results also from other differences of the stimuli. However, the VSDI response to MSs generated in the presence of either large stimuli: Gabor matrix—comprises of single Gabors (note that we used a single Gabor as a small stimulus), or natural faces and their scrambled version, was highly similar, and for both stimuli demonstrated a biphasic

response (Fig. 4). The fact that we observed a highly similar response for 2 remote categories of visual stimuli composed from very different features, support the notion that the activity difference between the small and large stimulus results from size difference rather than other differences. A possible explanation for the activity difference between small and large stimulus is as follows. Because the large stimulus was positioned in the visual field to retinotopically match the location of the imaged area and because it spanned several degrees of visual field, it evoked VSDI activation within the entire V1 imaged area. This led to high VSDI activity in most of the pixels in V1 before any MS. When an MS occurred, it was performed within the boundaries of stimulus, the MSs being much smaller than the visual stimulus. Thus, most of the neurons' RFs within the imaged area were activated by the visual stimulus before and after an MS. During the MS, the VSDI signal showed a transient induced by the image shift over the retina (Figs 3 and 4). In contrast, the local stimulus induced a local patch of activation in V1. Pixels in V1 directly activated by the visual stimulus showed a high activity before the MS onset, whereas pixels not activated by the visual stimulus had a low baseline activity. This caused very different neuronal activity before an MS. Following an MS, pixels activated by the Gabor stimulus showed high activity (neurons whose RF was activated by the new position of the Gabor stimulus) and pixels initially showing a high activity now decreased their response following the MS, as the RF left the stimulus. In addition, Supplementary Figure S2 shows that following an MS during a Gabor matrix presentation, the VSDI response of different sites either increased (as in site A, small stimulus, Fig. 2) or decreased (as in site B, small stimulus, Fig. 2) or showed other time courses of transient activation. The specific dynamics at each site depended on the amplitude of VSDI signal before and after the MS. When averaging across many pixels in V1 an averaged biphasic VSDI signal results (Figs 3 and 4, Supplementary Fig. S2).

The V2 area responded similarly to V1, with initial suppression followed by a transient increase, albeit with a delay (see also Leopold and Logothetis 1998). This suggests a central role for bottom-up processing in these areas. The biphasic response observed in V2 and V1 may reflect different temporal phases of visual perception during an MS.

The suppression observed with the large stimuli appears to begin prior to or immediately after an MS, too short a time for retinal influences, given the retinocortical delays. Possible explanations of studies similarly reporting presaccadic or pre-MS modulation of neural activity in visual areas (Leopold and Logothetis 1998; Martinez-Conde et al. 2002; Purpura et al. 2003; Rajkai et al. 2008; Bosman et al. 2009) include: 1) Rhythmic behavior of MSs can induce pre-MS modulation. An analysis of our data similar to that of Bosman et al. (2009) showed that longer intervals between successive eye movements significantly affected the pre-MS modulation. 2) Extra-retinal input to V1. Kagan et al. (2008) reported a prolonged extraretinal modulation, which thus did not appear to be a mirror image of short-lived motor commands (corollary discharges). However, extrastriate modulation during MSs is highly debated and was reported to be variable across animals (Kagan et al. 2008). To test for extraretinal modulation in our data, we calculated the VSDI response to MSs when the animal was fixating on a uniform gray screen. Whereas one animal showed clear VSDI modulation in this condition, the other did not, similar to Kagan et al. (2008). 3) Another option is that the VSDI signal before MSs reflects neural adaptation to a previously presented visual stimulus over scales of tens to hundreds of milliseconds. Martinez-Conde et al. (2006) have recently shown that visual fading was terminated by MSs. Our use of VSDI, emphasizing subthreshold population activity may highlight such neural adaptation processes. 4) Discrepancies with previous results may be due to VSDI emphasizing subthreshold population response, while previous studies used single or multiunit recordings. For example, our results partially agree with Bosman et al. (2009), who measured LFP that is a population signal, emphasizing synaptic input, and thus reminiscent of the VSDI signal.

The Relation between MS Amplitude and VSDI Modulation

We found a linear relation between the MS amplitude and the modulation of neuronal activity or VSDI signal derivative, as also reported by Armington and Bloom (1974), Dimigen et al. (2009), and an functional magnetic resonance imaging study by Tse et al. (2010). Tse et al. (2010) found that the blood oxygen level–dependent signal covaried with the size of voluntary small saccades within the amplitude range of MSs. Our results suggest that the modulation is profound mainly during the initial transient suppression, the amplitude of this suppression increasing as a function of MS size. The timing of this suppression did not depend on Ms size, supporting our assumption that the first 100 ms after MS onset are dedicated to stimulus displacement and not to perceptual purposes. The increase in VSDI modulation amplitude with MS size may arise as neurons in V1 become less responsive with increasing eye movement velocity (Battaglini et al. 1993). Finally, although we did not find a significant difference between the VSDI traces of different MSs amplitude before MS onset, it is possible that additional data will better clarify the weak trends observed before MS onset.

MSs Modulate Neural Synchronization

MSs may affect synchronization of neuronal activity across visual areas (Leopold and Logothetis 1998; see also Melloni et al. 2009). Martinez-Conde et al. (2000, 2002) further proposed that due to synchronization within levels of the processing hierarchy, spatial, and temporal summation is facilitated after each MS and then propagate to the next level of processing. Our results are in accordance with these studies: the average VSDI correlation maps in V1 showed increased synchronization within large neuronal populations early after MS onset. Increased synchronization in the VSDI signal reflects increased common dynamic changes of the VSDI signals across neural population (e.g., across different pixels). For example, a mutual increase of the VSDI signal or a mutual decrease in the VSDI signal in 2 pixels will lead to high synchronization level between these pixels. A decreased synchronization of the VSDI signal (e.g., ~200 ms after MS onset, Figs 7*B* and 8*A*) can reflect increased independent activity of pixels. For example, when 2 pixels who previously shared common dynamics, shift to a new state where they do not share a common dynamics but rather fluctuate randomly across a constant level of activation, the VSDI synchronization will decrease.

Synchronization within the gamma range in the LFP signal in the visual cortex in relation to MSs was recently reported by

Bosman et al. (2009). The V1 coherence analysis showed a rapid post-MS decrease followed by a transient increase in synchronization of the gamma band within the first 200 ms post-MS. Our correlation analysis on the VSDI signal also revealed changes in synchronization. However, unlike Bosman et al., we found that, during presentation of the large visual stimuli, synchronization increased significantly over most of the imaged V1 and V2 areas shortly after MS onset. For the local stimuli, early increased synchronization at the pre-MS activation site is related to the decreasing VSDI signal at this site. This was followed by an increased synchronization at the post-MS activation site related to the increasing VSDI signal here. The difference between our observations and those of Bosman et al. may stem from the fact that they measured LFP while we measured the VSDI signal. As we recently showed, the transfer function between the 2 signals is complex and frequency dependent (Gilad et al. 2008). Part of the temporal difference in synchronization that we measured may be related to the shorter time window in which we calculated synchronization (80 ms window), whereas Bosman et al. used a 200 ms window which can blur and smear out short correlation epochs.

Bosman et al. also reported a periodic pattern of synchronization in V1 (3–4 Hz, see also Melloni et al. 2009). We also found a rhythmic pattern of temporal synchronization in the VSDI signal, a decrease in synchronization starting −90 to −50 ms pre-MS followed by a large post-MS enhancement of synchronization peaking at 60–90 ms. This was followed by another epoch of decreased correlation. Although the periodic pattern may be related to the MS itself, it may also reflect the periodic appearance of MSs (Bosman et al. 2009). To address this issue, we studied the synchronization pattern in long traces that included single MSs, but our results were inconclusive, a periodic pattern almost disappearing in one animal while it was still weakly evident in the other.

Increased synchronization may account for the elevated perception threshold during an MS (Zuber and Stark 1966) or it may signal the arrival of new visual input (Leopold and Logothetis 1998; Martinez-Conde et al. 2000, 2002). The decreased synchronization during the pre-MS interval may be due to a relatively reduced mutual modulation among pixels in the VSDI signal (see explanation above). As the pre-MS interval reflects the last part of the drift eye movement epoch, the decreased synchronization may be linked to detailed image processing. Finally, we note that spatial smoothing increased the absolute value of correlation for the real and shuffle data, suggesting that the low correlation values are limited by signal-to-noise levels.

Visual Perception during MSs

We do not perceive the world moving during MSs, suggesting that compensatory mechanisms counter the motion signals generated by MSs (Murakami and Cavanagh 1998, 2001). This compensation may interfere with our ability to extract visual information just before and during MSs, thus reducing visual discrimination. Indeed, several recent studies have reported that reaction time (RT) is increased when an MS takes place close to stimulus onset or the GO signal (Rolfs et al. 2006; Bosman et al. 2009; Herrington et al. 2009; Kliegl et al. 2009). MSs occurring during very brief stimuli are associated with significantly reduced motion detection performance and increased RT (Herrington et al. 2009). The increased RT may indicate impaired visual processing during the execution of MS (but see Horowitz et al. 2007). Furthermore, MSs may also raise visual detection thresholds, that is, MSs suppression (Ditchburn 1955; Beeler 1967; Herrington et al. 2009; Martinez-Conde et al. 2009 but see Krauskopf and Gaarder 1966; Sperling 1990).

In conclusion, we found prominent neuronal modulation within 200 ms after MS onset. This modulation included a spatially segregated early decrease followed by an increase in neural activity for small stimuli or biphasic neural responses measured over most parts of the activated areas for larger stimuli. These changes were accompanied by increased synchronization just after the MS onset. This could imply that the suppressed activity may underlie the suppressed perception during MSs, as a result of the image movement over the retina. The late enhancement may facilitate the processing of new incoming image information, with the decreased synchronization reflecting epochs of stabilization and image analysis. A fully detailed image analysis can most likely be achieved with prolonged image stabilization over the retina (during the drift eye movement period). However, a prolonged period of stabilization may result in neural adaptation and image fading. Thus, these 2 processes probably balance each other throughout an MS generation (Melloni et al. 2009). Whether the activation transients or synchronization generated by MSs is important for visual perception remains to be tested in future experiments.

Supplementary Material

Supplementary material can be found at: http://www.cercor.oxfordjournals.org/

Funding

National Institute for Psychobiology in Israel (grant 238-07-08); Israel Science Foundation (grant 859/05).

Notes

We are grateful to Hadar Edelman and Ariel Gilad for their valuable help with the experiments. *Conflict of Interest*: None declared.

References

Angelucci A, Levitt JB, Walton EJ, Hupe JM, Bullier J, Lund JS. 2002. Circuits for local and global signal integration in primary visual cortex. J Neurosci. 22:8633–8646.

Arieli A, Grinvald A, Slovin H. 2002. Dural substitute for long-term imaging of cortical activity in behaving monkeys and its clinical implications. J Neurosci Methods. 114:119–133.

Arieli A, Shoham D, Hildesheim R, Grinvald A. 1995. Coherent spatiotemporal patterns of ongoing activity revealed by real-time optical imaging coupled with single-unit recording in the cat visual cortex. J Neurophysiol. 73:2072–2093.

Armington JC, Bloom MB. 1974. Relations between the amplitudes of spontaneous saccades and visual responses. J Opt Soc Am. 64:1263–1271.

Ayzenshtat I, Meirovithz E, Edelman H, Werner-Reiss U, Bienenstock E, Abeles M, Slovin H. 2010. Precise spatiotemporal patterns among visual cortical areas and their relation to visual stimulus processing. J Neurosci. 30:11232–11245.

Bair W, O'Keefe LP. 1998. The influence of fixational eye movements on the response of neurons in area MT of the macaque. Vis Neurosci. 15:779–786.

Battaglini PP, Galletti C, Fattori P. 1993. Functional properties of neurons in area V1 of awake macaque monkeys: peripheral versus central visual field representation. Arch Ital Biol. 131: 303–315.

Beeler GW, Jr. 1967. Visual threshold changes resulting from spontaneous saccadic eye movements. Vision Res. 7:769–775.
Bosman CA, Womelsdorf T, Desimone R, Fries P. 2009. A microsaccadic rhythm modulates gamma-band synchronization and behavior. J Neurosci. 29:9471–9480.
Bridgeman B. 1999. Neither strong nor weak space constancy is coded in striate cortex. Psychol Res. 62:261–265.
Bridgeman B, Palca J. 1980. The role of microsaccades in high acuity observational tasks. Vision Res. 20:813–817.
Collewijn H, Kowler E. 2008. The significance of microsaccades for vision and oculomotor control. J Vis. 8:20–21.
Cornsweet TN. 1956. Determination of the stimuli for involuntary drifts and saccadic eye movements. J Opt Soc Am. 46:987–993.
Cui J, Wilke M, Logothetis NK, Leopold DA, Liang H. 2009. Visibility states modulate microsaccade rate and direction. Vision Res. 49:228–236.
Dimigen O, Valsecchi M, Sommer W, Kliegl R. 2009. Human microsaccade-related visual brain responses. J Neurosci. 29:12321–12331.
Ditchburn RW. 1955. Eye-movements in relation to retinal action. Opt Acta Int J Opt. 1:171–176.
Dow BM, Snyder AZ, Vautin RG, Bauer R. 1981. Magnification factor and receptive field size in foveal striate cortex of the monkey. Exp Brain Res. 44:213–228.
Engbert R. 2006. Microsaccades: a microcosm for research on oculomotor control, attention, and visual perception. Prog Brain Res. 154:177–192.
Engbert R, Kliegl R. 2003. Microsaccades uncover the orientation of covert attention. Vision Res. 43:1035–1045.
Engbert R, Kliegl R. 2004. Microsaccades keep the eyes' balance during fixation. Psychol Sci. 15:431–436.
Engbert R, Mergenthaler K. 2006. Microsaccades are triggered by low retinal image slip. Proc Natl Acad Sci U S A. 103:7192–7197.
Gilad A, Leshem A, Meirovithz E, Werner-reiss U, Slovin H. 2008. Spatial coherence analysis reveals inter and intra areas synchrony among neuronal population in behaving monkeys. Abstract In: The 17th Annual Meeting of the Israel Society for Neuroscience (ISFN), Eilat, Israel.
Grinvald A, Lieke EE, Frostig RD, Hildesheim R. 1994. Cortical point-spread function and long-range lateral interactions revealed by real-time optical imaging of macaque monkey primary visual cortex. J Neurosci. 14:2545–2568.
Grinvald A, Shoham D, Shmuel A, Glaser D, Vanzetta I, Shtoyerman E, Slovin H, Sterkin A, Wijnbergen C, Hildesheim R, et al. 1999. In-vivo optical imaging of cortical architecture and dynamics. In: Windhorst U, Johansson H, editors. Modern techniques in neuroscience research. 1st ed. New York: Springer. p. 893–969.
Gur M, Beylin A, Snodderly DM. 1997. Response variability of neurons in primary visual cortex (V1) of alert monkeys. J Neurosci. 17:2914–2920.
Herrington TM, Masse NY, Hachmeh KJ, Smith JE, Assad JA, Cook EP. 2009. The effect of microsaccades on the correlation between neural activity and behavior in middle temporal, ventral intraparietal, and lateral intraparietal areas. J Neurosci. 29:5793–5805.
Horowitz TS, Fine EM, Fencsik DE, Yurgenson S, Wolfe JM. 2007. Fixational eye movements are not an index of covert attention. Psychol Sci. 18:356–363.
Kagan I, Gur M, Snodderly DM. 2008. Saccades and drifts differentially modulate neuronal activity in V1: effects of retinal image motion, position, and extraretinal influences. J Vis. 8:19–25.
Kliegl R, Rolfs M, Laubrock J, Engbert R. 2009. Microsaccadic modulation of response times in spatial attention tasks. Psychol Res. 73:136–146.
Kowler E, Steinman RM. 1979. Miniature saccades: eye movements that do not count. Vision Res. 19:105–108.
Kowler E, Steinman RM. 1980. Small saccades serve no useful purpose: reply to a letter by R.W. Ditchburn. Vision Res. 20:273–276.
Krauskopf UG, Gaarder K. 1966. Lack of inhibition during involuntary saccades. Am J Psychol. 79:73–81.
Laubrock J, Engbert R, Rolfs M, Kliegl R. 2007. Microsaccades are an index of covert attention: commentary on Horowitz, Fine, Fencsik, Yurgenson, and Wolfe (2007). Psychol Sci. 18:364–366.
Leopold DA, Logothetis NK. 1998. Microsaccades differentially modulate neural activity in the striate and extrastriate visual cortex. Exp Brain Res. 123:341–345.
Livingstone MS, Freeman DC, Hubel DH. 1996. Visual responses in V1 of freely viewing monkeys. Cold Spring Harb Symp Quant Biol. 61:27–37.
MacEvoy SP, Hanks TD, Paradiso MA. 2008. Macaque V1 activity during natural vision: effects of natural scenes and saccades. J Neurophysiol. 99:460–472.
Martinez-Conde S. 2006. Fixational eye movements in normal and pathological vision. Prog Brain Res. 154:151–176.
Martinez-Conde S, Macknik SL, Hubel DH. 2000. Microsaccadic eye movements and firing of single cells in the striate cortex of macaque monkeys. Nat Neurosci. 3:251–258.
Martinez-Conde S, Macknik SL, Hubel DH. 2002. The function of bursts of spikes during visual fixation in the awake primate lateral geniculate nucleus and primary visual cortex. Proc Natl Acad Sci U S A. 99:13920–13925.
Martinez-Conde S, Macknik SL, Hubel DH. 2004. The role of fixational eye movements in visual perception. Nat Rev Neurosci. 5:229–240.
Martinez-Conde S, Macknik SL, Troncoso XG, Dyar TA. 2006. Microsaccades counteract visual fading during fixation. Neuron. 49:297–305.
Martinez-Conde S, Macknik SL, Troncoso XG, Hubel DH. 2009. Microsaccades: a neurophysiological analysis. Trends Neurosci. 32:463–475.
Meirovithz E, Ayzenshtat I, Bonneh YS, Itzhack R, Werner-Reiss U, Slovin H. 2010. Population response to contextual influences in the primary visual cortex. Cereb Cortex. 20:1293–1304.
Melloni L, Schwiedrzik CM, Rodriguez E, Singer W. 2009. (Micro)-Saccades, corollary activity and cortical oscillations. Trends Cogn Sci. 13:239–245.
Motter BC, Poggio GF. 1990. Dynamic stabilization of receptive fields of cortical neurons (VI) during fixation of gaze in the macaque. Exp Brain Res. 83:37–43.
Murakami I, Cavanagh P. 1998. A jitter after-effect reveals motion-based stabilization of vision. Nature. 395:798–801.
Murakami I, Cavanagh P. 2001. Visual jitter: evidence for visual-motion-based compensation of retinal slip due to small eye movements. Vision Res. 41:173–186.
Nachmias J. 1959. Two-dimensional motion of the retinal image during monocular fixation. J Opt Soc Am. 49:901–908.
Otero-Millan J, Troncoso XG, Macknik SL, Serrano-Pedraza I, Martinez-Conde S. 2008. Saccades and microsaccades during visual fixation, exploration, and search: foundations for a common saccadic generator. J Vis. 8:1–18.
Purpura KP, Kalik SF, Schiff ND. 2003. Analysis of perisaccadic filed potentials in the occipitotemporal pathway during active vision. J Neurophysiol. 90:3455–3478.
Rajkai C, Lakatos P, Chen CM, Pincze Z, Karmos G, Schroeder CE. 2008. Transient cortical excitation at the onset of visual fixation. Cereb Cortex. 18:200–209.
Reppas JB, Usrey WM, Reid RC. 2002. Saccadic eye movements modulate visual responses in the lateral geniculate nucleus. Neuron. 35:961–974.
Riggs LA, Ratliff F, Cornsweet JC, Cornsweet TN. 1953. The disappearance of steadily fixated visual test objects. J Opt Soc Am. 43:495–501.
Rolfs M. 2009. Microsaccades: small steps on a long way. Vision Res. 49:2415–2441.
Rolfs M, Engbert R, Kliegl R. 2004. Microsaccade orientation supports attentional enhancement opposite a peripheral cue: commentary on Tse, Sheinberg, and Logothetis (2003). Psychol Sci. 15:705–707.
Rolfs M, Kliegl R, Engbert R. 2008. Toward a model of microsaccade generation: the case of microsaccadic inhibition. J Vis. 8:5–23.
Rolfs M, Laubrock J, Kliegl R. 2006. Shortening and prolongation of saccade latencies following microsaccades. Exp Brain Res. 169: 369–376.
Rucci M, Desbordes G. 2003. Contributions of fixational eye movements to the discrimination of briefly presented stimuli. J Vis. 3:852–864.

Rucci M, Iovin R, Poletti M, Santini F. 2007. Miniature eye movements enhance fine spatial detail. Nature. 447:851–854.
Schira MM, Tyler CW, Breakspear M, Spehar B. 2009. The foveal confluence in human visual cortex. J Neurosci. 29:9050–9058.
Schira MM, Wade AR, Tyler CW. 2007. Two-dimensional mapping of the central and parafoveal visual field to human visual cortex. J Neurophysiol. 97:4284–4295.
Shoham D, Glaser DE, Arieli A, Kenet T, Wijnbergen C, Toledo Y, Hildesheim R, Grinvald A. 1999. Imaging cortical dynamics at high spatial and temporal resolution with novel blue voltage-sensitive dyes. Neuron. 24:791–802.
Shtoyerman E, Arieli A, Slovin H, Vanzetta I, Grinvald A. 2000. Long-term optical imaging and spectroscopy reveal mechanisms underlying the intrinsic signal and stability of cortical maps in V1 of behaving monkeys. J Neurosci. 20:8111–8121.
Skavenski AA, Hansen RM, Steinman RM, Winterson BJ. 1979. Quality of retinal image stabilization during small natural and artificial body rotations in man. Vision Res. 19:675–683.
Skavenski AA, Robinson DA, Steinman RM, Timberlake GT. 1975. Miniature eye movements of fixation in rhesus monkey. Vision Res. 15:1269–1273.
Slovin H, Arieli A, Hildesheim R, Grinvald A. 2002. Long-term voltage-sensitive dye imaging reveals cortical dynamics in behaving monkeys. J Neurophysiol. 88:3421–3438.
Snodderly DM, Kagan I, Gur M. 2001. Selective activation of visual cortex neurons by fixational eye movements: implications for neural coding. Vis Neurosci. 18:259–277.
Sperling G. 1990. Comparison of perception in the moving and stationary eye. Rev Oculomot Res. 4:307–351.
Tootell RB, Switkes E, Silverman MS, Hamilton SL. 1988. Functional anatomy of macaque striate cortex. II. Retinotopic organization. J Neurosci. 8:1531–1568.
Tse PU, Baumgartner FJ, Greenlee MW. 2010. Event-related functional MRI of cortical activity evoked by microsaccades, small visually-guided saccades, and eyeblinks in human visual cortex. Neuroimage. 49:805–816.
Van Essen DC, Anderson CH, Felleman DJ. 1992. Information processing in the primate visual system: an integrated systems perspective. Science. 255:419–423.
Wurtz RH. 2008. Neuronal mechanisms of visual stability. Vision Res. 48:2070–2089.
Yuval-Greenberg S, Tomer O, Keren AS, Nelken I, Deouell LY. 2008. Transient induced gamma-band response in EEG as a manifestation of miniature saccades. Neuron. 58:429–441.
Zuber BL, Stark L. 1965. Microsaccades and the velocity-amplitude relationship for saccadic eye movements. Science. 150:1459–1460.
Zuber BL, Stark L. 1966. Saccadic suppression: elevation of visual threshold associated with saccadic eye movements. Exp Neurol. 16:65–79.